

RESOLUTION IMPROVEMENT FILTER FOR SONAR RETURNS⁽¹⁾

A. DYKA

Technical University of Gdańsk, Institute of Telecommunications
(80-952 Gdańsk, ul. Majakowskiego 11/12)

The concern of this paper is the Single Pulse Resolution Filter — SPRF, which is capable of resolving near-rectangular overlapping pulses. The reason for assuming such pulses is that despite the attractive properties of matched filter pulse compression most operational sonar systems continue to use a finite-length rectangular pulse of constant frequency. The task of the SPRF in such system is to improve the short-range resolution and the target detectability in reverberation. The SPRF here discussed has been synthesized on the basis of the ideal deconvolution filter concept by using the semi-heuristic method of the transformation and the supplementing of input signal spectrum. In order to evaluate the SPRF performance three performance indices have been defined, namely the resolution improvement ratio, the degradation in the output signal-to-noise ratio compared to the maximum which is attainable in the matched filter case, and the processing gain against reverberation. The tradeoffs between the performance indices given in an analytic form have been presented and briefly discussed. The results of tests with the SPRF, both in the laboratory and in sea trials are reported. The first of them proves the resolution capability of the SPRF in the case of two, noise-contaminated overlapping returns. The sea trials were carried out during the FAO sponsored BIOMASS First International Biological Experiment, (FIBEX 81), programme in Antarctica on board the Polish research vessel "Profesor Siedlecki". A number of echograms produced originally by the Simrad SK-120 echosounder and after having the received signal envelope filtered with the SPRF were recorded simultaneously. Two samples of such echograms recorded on the Brazilian Shelf in April 1981 which show the favourable impact of the SPRF on the picture quality are presented. Finally, the drawbacks of the SPRF are mentioned.

1. Introduction

A problem of considerable importance in many areas of science and technology is the unambiguous resolution of multiple overlapping pulses. General solutions to this problem include deconvolution, (inverse) filtering, (e.g., SENMOTO and CHILDERS,

⁽¹⁾ This paper was presented at International Symposium on Fisheries Acoustics, June 22-26, 1987, Seattle, Washington, USA.

[10]), matched filter pulse compression, (e.g., COOK and BERNFELD, [2], cepstrum analysis, (e.g., OPPENHEIM and SCHAFER [8]), mismatched filtering, (e.g., EVANS and FORTMANN [6]), and the "moments" algorithms, (BAUM 1975; SANDHU and AUDEH [1, 9]). A particular case occurs in sonar and radar where the shape of the transmitted pulse is known. Then, the matched filter pulse compression is superior to any linear method. However, as the pulse compression signals are wideband ones their direct application to a conventional sonar system is difficult, due to the narrow bandwidth of transmitting transducers and the frequency dependent attenuation of ultrasonic waves in sea. For that reason the practically obtainable ratio of signal compression is not expected to exceed 100. This fact and the increased cost and complexity of pulse compression systems as compared to conventional options means that most commercially available sonar systems continue to use a finite-length rectangular pulse of constant frequency. On the other hand, the use of long pulses in such systems, necessary to obtain the desired long-range target detection contributes to poor resolution in range and poor detectability of targets in reverberation. One may partly resolve these conflicting demands by using long pulses, so that detection in range is not compromised and by applying special receiver filtering techniques, which partly recover the short-range resolution and the detectability of targets in reverberation.

The concern of this paper is the Single Pulse Resolution Filter, which from now on will be referred to as the SPRF, intended for use in conventional sonar systems employing a finite-length rectangular pulse. The task of this filter is to improve the short-range resolution and the detectability of targets in reverberation.

2. Formulation and solution to the filtering problem

Prior to the formulation of the filtering problem the input signal is to be defined. A reasonable model of a single return is a near-rectangular, trapezoidal pulse, which can be modelled as the output signal of a low-pass filter, excited by a rectangular pulse. This low-pass filter represents the overall bandwidth of a sonar system and its cut-off frequency is basically limited by the bandwidth of the transmitting transducer. The usual design criterion of maximizing the system output signal-to-noise ratio means, that in practice the matched receiver is mainly responsible for the most severe bandwidth limitation, and converts the envelope of a single return into a near-triangular pulse. However, as from the practical standpoint one can easily manipulate the receiver bandwidth, while in the case of the transmitting transducer one can not do so, it is reasonable to assume that the real, physical limitation of the overall bandwidth is almost entirely due to the transmitting transducer.

Despite the above considerations it is assumed here that the envelope of a single return is a rectangular pulse of the length T . Not only does such an assumption simplify dramatically the design procedure but as is shown later, the results achieved also apply to the more realistic models of the return envelopes considered above.

Basically, an improvement in range resolution can be achieved by filtering which "compresses" the return of the length T into another, possibly the shortest pulse. The ratio of the pulse-lengths prior to the compression and after the compression, respectively is usually referred to as the compression ratio. Taking into account the above assumption about the input signal the best possible filter of this kind should be capable of transforming the rectangular pulse of the length T into a Dirac's delta distribution, (see Fig. 1). Actually, this is a definition of an ideal deconvolution filter. Having formulated the filtering problem in this way we find that the deconvolution filter shown in Fig. 1 is a non-causal and nonlinear one. Unfortunately, the coherent body of knowledge concerning the linear processing of signals has no counterpart in the treatment of nonlinear signal processes. Therefore, any feasible solution of a nonlinear problem may be considered as a reasonable one, although it is usually difficult to prove whether such a solution is an "optimum" one in any sense. Non-causality of the filter is only a minor problem as it can be removed by an appropriate delaying the output signal.

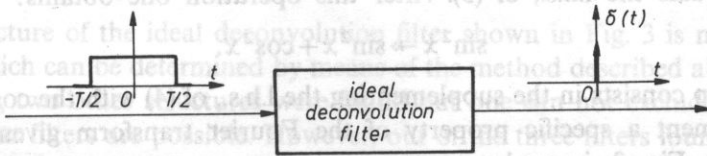


FIG. 1. Definition of the deconvolution filter for a rectangular pulse of the length T . $\delta(t)$ — denotes Dirac's delta distribution

In order to determine a feasible structure of the deconvolution filter shown in Fig. 1 the semi-heuristic method of the transformation and the supplementing of the input signal spectrum in such a way as to obtain the spectrum of the desired output signal was proposed by ДУКА, [3]. The transformation and supplementing of the spectrum refer to linear and nonlinear operations, respectively, which are performed on the corresponding signals in the time domain. To illustrate the method briefly, consider the spectrum of the input rectangular pulse as the $\frac{\sin x}{x}$, $x = \omega T/2$, where: ω — is angular frequency, T — is the pulse-length, and the spectrum of the desired output pulse is 1. Then, we can symbolize the filtering procedure as;

$$\frac{\sin x}{x} \rightarrow 1, \quad (1)$$

where the double arrow denotes all operations performed upon the $\frac{\sin x}{x}$ spectrum, which transform it into 1. The crucial point is, that every operation performed upon

the spectrum in the frequency domain must correspond to its feasible counterpart in the time domain. Consequently, we can rewrite (1) as:

$$\frac{\sin x}{x} \rightarrow \sin^2 x + \cos^2 x. \quad (2)$$

The first step in transforming the spectrum on the left hand side, (l.h.s.), of (2) into the spectrum on the right hand side, (r.h.s.), consists in removing the denominator from the l.h.s., by multiplying the l.h.s., by jx , where $j = \sqrt{-1}$. In the time domain it corresponds to the operation of differentiation. Thus we get:

$$j \sin x \rightarrow \sin^2 x + \cos^2 x. \quad (3)$$

The next step is to transform the $j \sin x$ l.h.s., spectrum into the $\sin^2 x$ spectrum. This can be obtained by multiplying the l.h.s., of (3) by $-j \sin x$, which in the time domain corresponds to the filtering with a linear filter, whose impulse response equals $h(t) = \delta(t - T/2) - \delta(t + T/2)$, where $\delta(\cdot)$ denotes Dirac's delta distribution. It is worth noting that this operation is actually the filtering, matched to the signal whose spectrum equals the l.h.s., of (3). After this operation one obtains:

$$\sin^2 x \rightarrow \sin^2 x + \cos^2 x. \quad (4)$$

The final step consists in the supplementing the l.h.s., of (4) with the $\cos^2 x$ function. At this moment a specific property of the Fourier transform given by (5) and illustrated in Fig. 2, is used;

$$|F^{-1}(\sin^2 x)| = F^{-1}(\cos^2 x). \quad (5)$$

where the $|\cdot|$ bracket denotes the absolute value operation performed upon a signal in the time domain, and F^{-1} denotes the Fourier inverse transform. The three steps described by (3) to (5) enable us to sketch immediately the structure of the

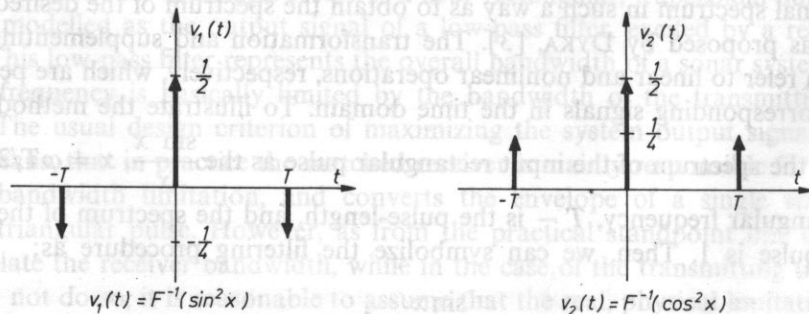


FIG. 2. Illustration of a specific property of the Fourier transform given by formula (5). $v_1(t)$ — denotes the absolute value circuit input signal in the deconvolution filter shown in Fig. 3. $v_2(t)$ — denotes the absolute value circuit output signal in the deconvolution filter shown in Fig. 3. F^{-1} — denotes the Fourier inverse transform. T — denotes the length of a sounding pulse. $x = \omega T/2$, where ω — denotes the radian frequency

deconvolution filter desired, as shown in Fig. 3. Remarkably the filter shown in Fig. 3 is not causal due to the factor $\delta(t + T/2)$ appearing in the impulse response $h(t)$. However, it can be coerced to be so by introducing the delay of $T/2$ in $h(t)$, which results only in delaying the output signal.

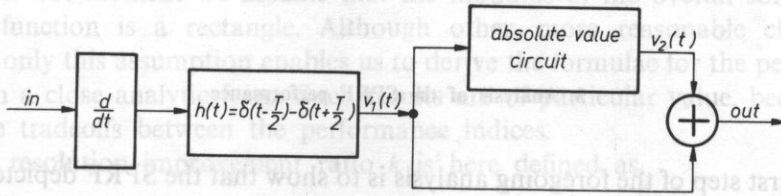


FIG. 3. Ideal deconvolution filter for a rectangular pulse of the length T . $\frac{d}{dt}$ — denotes operation of differentiation, $h(t)$ — denotes impulse response of a linear filter, $v_1(t)$ — denotes the absolute value circuit input signal, $v_2(t)$ — denotes the absolute value circuit output signal, $\delta(\cdot)$ — denotes Dirac's delta distribution, T — denotes the length of a sounding pulse

The structure of the ideal deconvolution filter shown in Fig. 3 is not the only possibility which can be determined by means of the method described above. Apart from this one, two other structures were found but one can not exclude that some other nonlinear filters are possible. However, out of the three filters found, the filter shown in Fig. 3 yields the maximum signal-to-noise ratio and therefore it was chosen for further examinations. One can show that the deconvolution filter depicted in Fig. 3 is equivalent to the filter shown in Fig. 4. The latter from now on will be referred to as the Single Pulse Resolution Filter — SPRF. As can be seen in Fig. 4 the SPRF consists of three basic elements namely the differentiator, the transversal filter, and

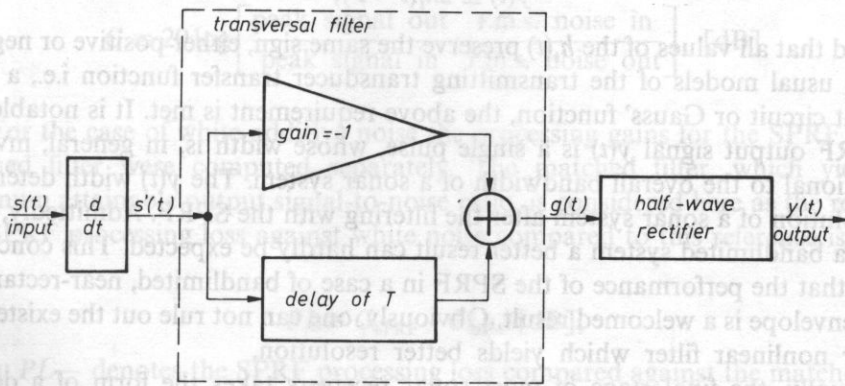


FIG. 4. SPRF circuit diagram, $s(t)$ — denotes the SPRF input signal, $s'(t)$ — denotes the differentiator output signal, $g(t)$ — denotes the transversal filter output signal, $y(t)$ — denotes the SPRF output signal, T — denotes the length of a sounding pulse

the half-wave rectifier. The first two are the linear circuits, while the third one, nonlinear, is a threshold circuit with the threshold voltage of zero volts. It should be pointed out, that the linear part of the SPRF resembles to some extent the pulse-length discriminator, (LAWSON and UHLENBECK [7]), and the High-Pass Sidelobe Reduction Filter, (EVANS and FORTMANN [6]).

3. Analysis of the SPRF performance

The first step of the foregoing analysis is to show that the SPRF depicted in Fig. 4 can be successfully applied to the near-rectangular, trapezoidal input pulses. Such pulses, as already mentioned in the preceding section, can be assumed as more reasonable models of the sonar return envelope than a rectangular pulse. As has also been pointed out, the transmitting transducer is the main contributor to the limitation of the overall system bandwidth. Taking into account that transmitting transducers are as a rule narrowband ones, one can show that the derivative $s'(t)$ of a single return envelope $s(t)$ is given a

$$s'(t) \cong h_t(t) - h_t(t - T), \quad (6)$$

where $h_t(t)$ denotes the impulse response envelope of a transmitting transducer. Actually, the signal given by (6) is the output signal of the differentiator in the SPRF. One may easily find that the output signal $g(t)$ of the transversal filter in the SPRF equals:

$$g(t) \cong 2h_t(t - T) - h_t(t) - h_t(t - 2T). \quad (7)$$

Hence, the output signal $y(t)$ of the SPRF equals;

$$y(t) \cong 2h_t(t - T), \quad (8)$$

provided that all values of the $h_t(t)$ preserve the same sign, either positive or negative. For the usual models of the transmitting transducer transfer function i.e., a single resonant circuit or Gauss' function, the above requirement is met. It is notable, that the SPRF output signal $y(t)$ is a single pulse, whose width is, in general, inversely proportional to the overall bandwidth of a sonar system. The $y(t)$ width determines the resolution of a sonar system after the filtering with the SPRF. Admittedly, in the case of a bandlimited system a better result can hardly be expected. This conclusion means, that the performance of the SPRF in a case of bandlimited, near-rectangular return envelope is a welcomed result. Obviously, one can not rule out the existence of another nonlinear filter which yields better resolution.

Usually, the final stage of most sonar receivers takes the form of a decisive threshold circuit, which basically is a switch that switches "on" when the signal amplitude exceeds a certain pre-fixed value. Therefore, if the SPRF is followed by such a threshold circuit, which actually doubles the task of the SPRF half-wave

rectifier, then the latter can be omitted. Consequently, the SPRF reduces to the linear circuit consisting of the differentiator and the transversal filter only. This conclusion enables us to estimate the SPRF performance indices namely the resolution improvement ratio, the processing loss against white noise compared to the matched filter case, and the processing gain against reverberation, using the linear filtering theory. At this moment we assume that the modulus of the overall sonar system transfer function is a rectangle. Although other, more reasonable choices are possible, only this assumption enables us to derive the formulae for the performance indices in a close analytic form. Such results are of particular value, because they show the tradeoffs between the performance indices.

The resolution improvement ratio k is here defined as,

$$k \equiv \frac{T}{t_0}, \quad (9)$$

where: T — is the pulse-length of the sounding pulse, t_0 — is the pulse-length of the SPRF response to the envelope of a single return.

Notably, k can be also interpreted as the compression ratio defined in Section 2. The assumption about the rectangular shape of the overall system transfer function implies that the response of the SPRF to the input rectangular envelope is the $\frac{\sin x}{x}$ type of function. Having defined t_0 as the width of the "mainlobe" in the SPRF response, we get the following;

$$k = \frac{1}{2} WT, \quad (10)$$

where W denotes the overall bandwidth of a sonar system.

The processing gains were computed using the following definition:

$$G \equiv 20 \log \left[\frac{\text{peak signal out} \cdot \text{r.m.s. noise in}}{\text{peak signal in} \cdot \text{r.m.s. noise out}} \right], \quad [\text{dB}] \quad (11)$$

For the case of white additive noise the processing gains for the SPRF and the matched filter were computed separately. The matched filter, which yields the maximum attainable output signal-to-noise ratio, is considered here as the reference. The SPRF processing loss against white noise compared to this reference is defined as:

$$PL \equiv G_{\text{SPRF}} - G_{\text{MF}}, \quad [\text{dB}], \quad (12)$$

where: PL — denotes the SPRF processing loss compared against the matched filter, G_{SPRF} — denotes the processing gain of the SPRF, G_{MF} — denotes the processing gain of the matched filter.

Routine transformations yield a rather complicated analytic formula for the PL

versus k . However, for $k > 3$ this formula can be well approximated by the asymptotic value it converges to, given as, (DYKA, [3]):

$$PL \cong -10 \log k - 2.2, \text{ [dB]}, \quad (13)$$

In order to estimate the processing gain against reverberation it was assumed that the process of reverberation can be modelled as the convolution of a transmitted sounding pulse with a series of Poisson impulses of random amplitudes. This assumption enables us to derive the formula for the power spectrum of the reverberation squared envelope, and consequently, the processing gain against reverberation G_r , as, (DYKA [3]):

$$G_r \cong 10 \log k - 2.1, \text{ [dB]}. \quad (14)$$

This result is basically consistent with conclusions that can be drawn from the phenomenological model of reverberation, (URICK, [11]). According to this model the reverberation level is inversely proportional to the return pulse-length. Therefore, if the SPRF "compresses" the return pulse-length k times then, at the same time it reduces the reverberation level by the same factor. Formulae (10), (13), and (14) show the tradeoffs between the SPRF performance indices. For a given pulse-length T the improvement in resolution expressed by k , (10), and the improvement in target detectability in reverberation, expressed by G_r , (14), do increase with increasing overall bandwidth of a sonar system. At the same time the output signal-to-noise ratio compared to the matched filter case, (expressed by PL , (13)), decreases by the same factor. So, the degradation of the output signal-to-noise ratio can be considered as the price which is to be paid for the "profits" expressed by an improvement in both resolution and target detectability in reverberation.

4. Experiments

With reference to Fig. 4 an analogue model of the SPRF has been constructed. As a delay line the Mullard TDA 1022, CCD integrated circuit has been used. Other elements are standard integrated circuits. First, the SPRF was tested in a laboratory using a return simulator delivering two 1 ms, low-pass filtered, ($f_c = 10$ kHz), rectangular, overlapping pulses. The CRT records in Fig. 5a and 5b show the following: the SPRF input signal (i) and the SPRF output signal (ii), noise free and contaminated by noise, respectively. Remarkably, the input signal, consists of two closely overlapping pulses, which at the presence of noise could not be resolved. In the output signal however, one may distinguish two dominating peaks, which indicate the appearance of two pulses in the input signal.

The sea trials were carried out during the FAO sponsored BIOMASS First International Biological Experiment, (FIBEX 81), programme in Antarctica on board the Polish research vessel "Profesor Siedlecki" in 1981. The parameters and

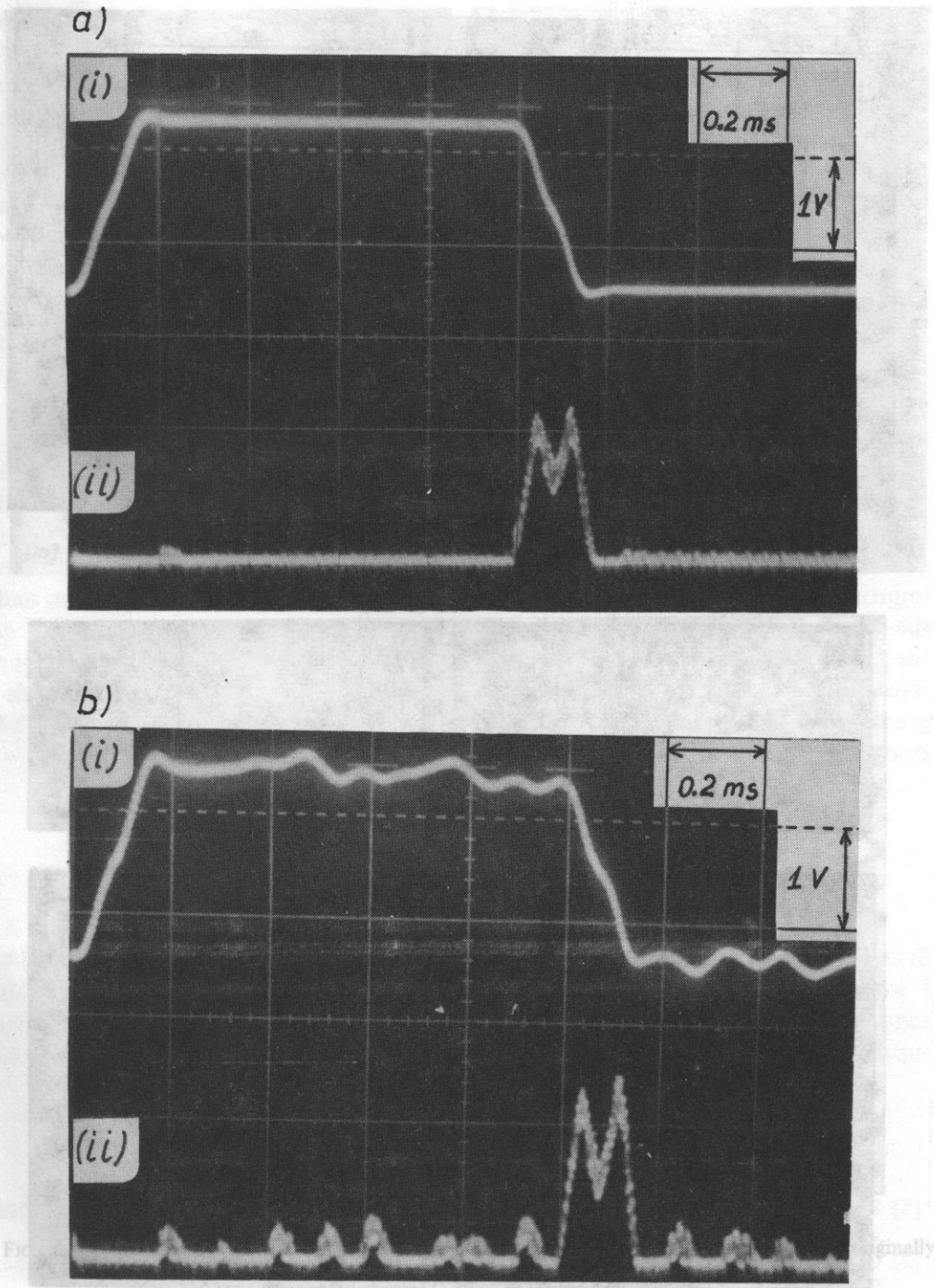


FIG. 5. CRT record of the SPRF input signal, (i) and the output signal, (ii), a — input signal free of noise, b — input signal contaminated by noise

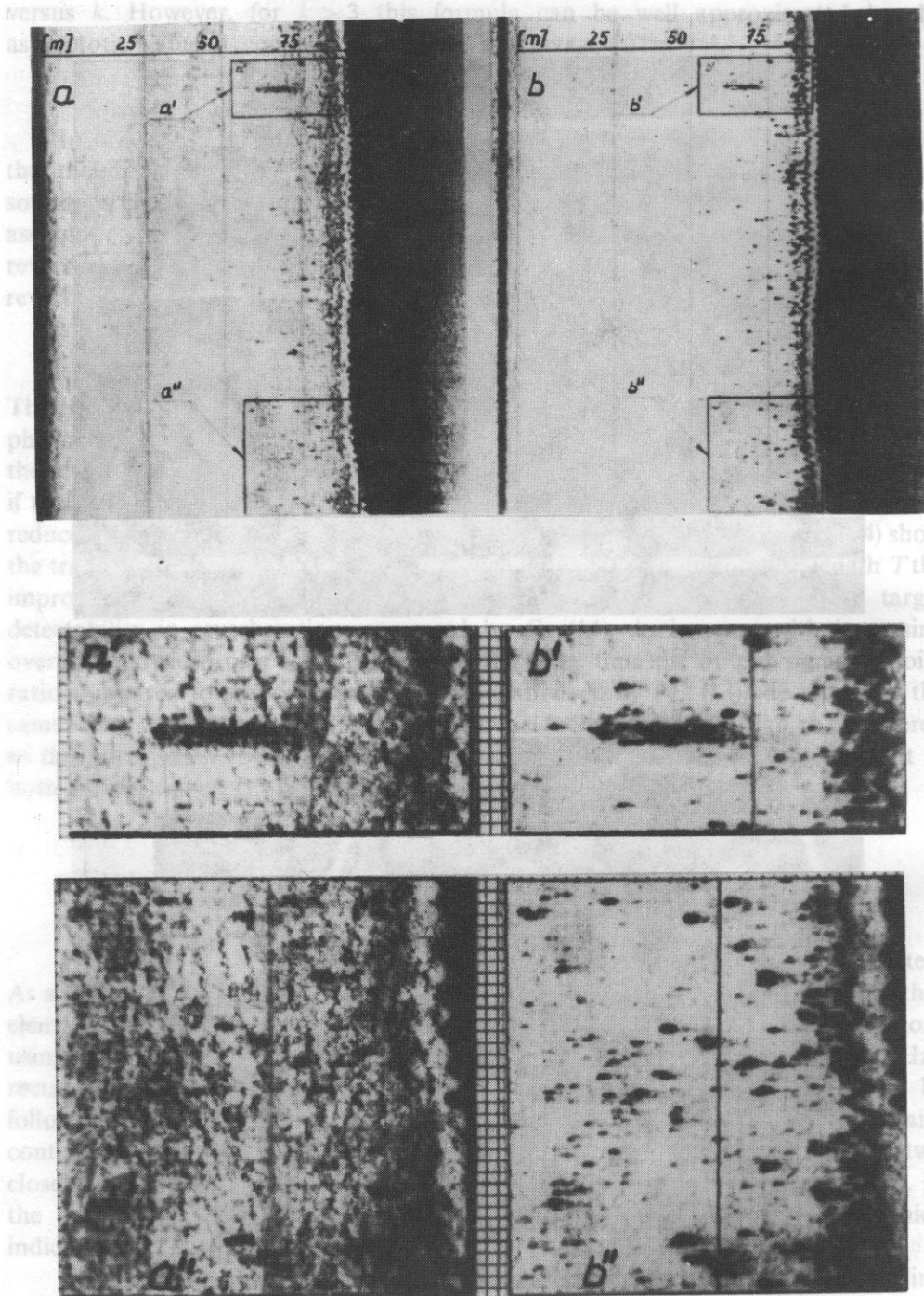


FIG. 6. Echogram of a medium density multiple target environment Brazilian Shelf. a, a', a'' — originally recorded by the echosounder; b, b', b'' — recorded with the use of the SPRF

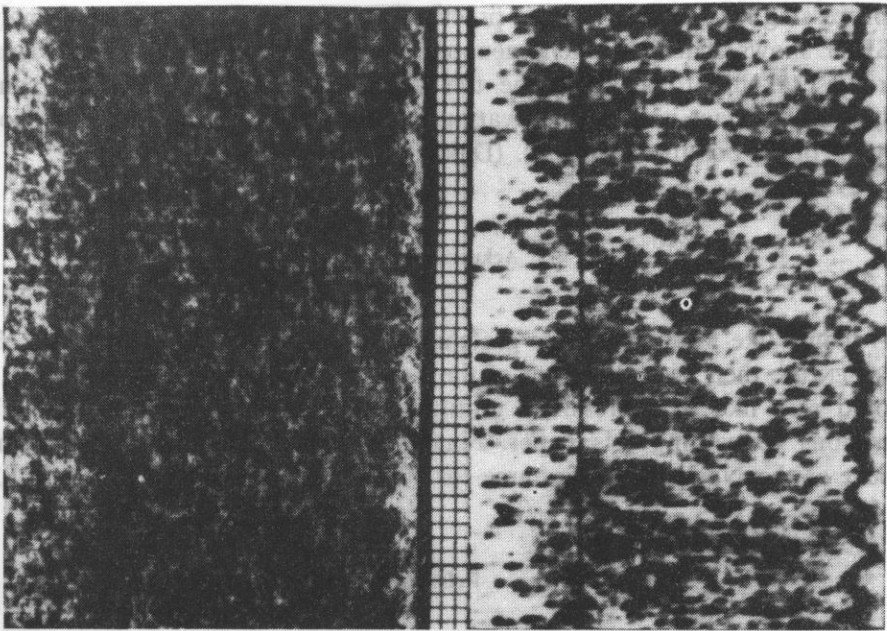
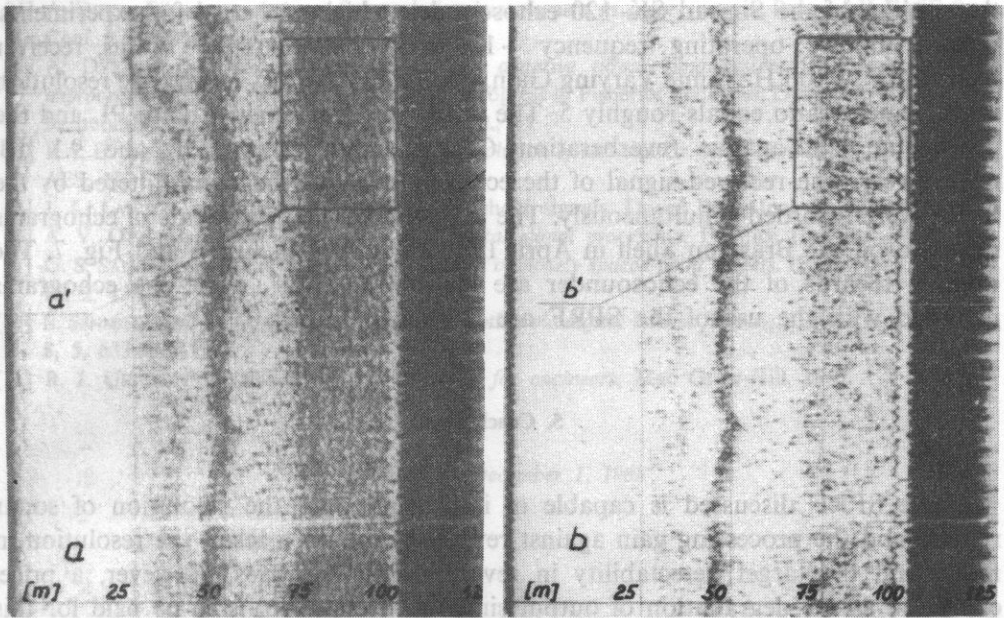


FIG. 7. Echogram of a high density multiple target environment, Brazilian Shelf. a, a' — originally recorded by the echosounder; b, b' — recorded with the use of the SPRF

- [1] R. F. BAUM, A novel algorithm for resolution of point targets IEEE Trans. on AES, 11, 6, 1260-1268, 1975.
- [2] G. E. L. Press, New York-London 1967.
- [3] A. DYKA, A model of filtering for resolution improvement in sonar systems, Ph. D. thesis (in Polish) 1984.

the settings of the Simrad SK-120 echosounder, which was used for experiments, were as follows: operating frequency - 120 KHz, pulse-length - 1 ms, receiver bandwidth - 10 kHz, Time Varying Gain, TVG), - 20 log R . Hence, the resolution improvement ratio equals roughly 5. The processing loss against noise PL and the processing gain against reverberation G_r , are roughly -9.2 dB and 9.1 dB, respectively. The received signal of the echosounder and the signal filtered by the SPRF were recorded simultaneously. The samples showing fragments of echograms recorded on the Brazilian Shelf in April 1981 are shown in Fig. 6 and Fig. 7. The original records of the echosounder are marked a, a', a'', while the echograms recorded with the use of the SPRF are marked b, b', b''.

5. Conclusions

The SPRF discussed is capable of improving both the resolution of sonar returns and the processing gain against reverberation. As a result the resolution in range and the target detectability in reverberation improves. However, a price, expressed as the degradation of output signal-to-noise ratio, is to be paid for this improvement. The tradeoff between the processing gain against reverberation and the processing loss against noise is practically equivalent. More detailed analysis of the SPRF shows, that if the phenomenon of mutual interference between overlapping returns is taken into account, the the SPRF performance undergoes some degradation. This fact was the motivation for developing an improved version and studying other possible solutions. (Dyka [4], [5]).

Acknowledgements

I would like to acknowledge gratefully the practical support given by Noel A. SVENDSEN the then Vice President of the Laitram Corporation, Boston, MA, USA. I would also like to express my gratitude to Prof. Zenon JAGODZINSKI for his suggestions concerning this paper. Finally, I would like to notify the financial support of the National Programme for Fundamental Research C.P.B.P. 02.16.4.

References

- [1] R. F. BAUM, *A novel algorithm for resolution of point targets*, IEEE Trans. on AES, 11, 6, 1260-1268 1975.
- [2] C. E. COOK and M. BERNFELD, *Radar signals - an introduction to theory and application*, Academic Press, New York-London 1967.
- [3] A. DYKA, *A model of filtering for resolution improvement in sonar systems*, Ph. D., thesis (in Polish) 1984.

recorded by the echosounder, b, b', b'' - recorded with the use of the SPRF

- [4] A. DYKA, *Filtering techniques for resolution improvement in sonar systems*, Proc. of II FASE Spec. Conf. 221-227 Madrid 1987.
- [5] A. DYKA, *Laboratory experiments with an adaptive thresholding system for range resolution improvement in sonar*, accepted for the Conf. Progress in Fisheries Acoustics, Lowestoft, UK, 1988, to be published in Proc. of the Inst. of Acoust., 11
- [6] R. J. EVANS and T. E. FORTMANN, *Optimal resolution of rectangular pulses in noise*, IEEE Trans., on AES, 11, 3, 372-379 (1975).
- [7] J. L. LAWSON and G. E. UHLENBECK, *Threshold signals*, Dover Publ. Inc., New York 1965.
- [8] A. V. OPPENHEIM and R. W. SCHAFER, *Digital signal processing*, Prentice Hall Inc., 1975.
- [9] G. S. SANDHU and N. F. AUDEH, *Measurement of closely spaced point targets*. IEEE Trans., on AES, 16, 2, 138-143 1980.
- [10] S. SENMOTO and D. G. CHILDERS, *Signal resolution via digital inverse filtering*, IEEE Trans., on AES, 8, 5, 633-640 1972.
- [11] R. J. URICK, *Principles of underwater sound for engineers*, Mac Graw-Hill, 1967.

Ultrasonic Department, Institute of Fundamental Technological Research, Polish Academy of Sciences, ul. P. Curie 21, 01-066 Warszawa, Poland

Received on December 1, 1988

The authors investigated detectability of calcifications by means of shadow and echo methods for 5 MHz frequency. Computing the ultrasonic field distribution around a rigid sphere they determined the shadow range and hence the detectability condition for calcification diameter $\phi \geq 3$ mm. For the echo method former investigations were continued improving the measurement technique and expanding the analysis. To determine the tissue signal background level measurements were performed on 82 breasts of healthy premenopausal women. The boundaries of various tissues and inhomogeneities within cause interfering background and its level limits the detectability. The measurement results, confirmed statistically, were used for detectability determination in normal breast tissues (attenuation 1.1 dB/cm MHz). The calculations show that the minimum diameter of a detectable calcification $\phi = 0.4$ mm for a normal breast. JACKSON et al. [18] and KASIMO [19,20] have demonstrated calcifications 0.1-0.5 mm in dia with frequencies of 4 and 7.5 MHz. These results are in general agreement with our theory if one takes into account the high (SD = 8 dB) scattering of the signal background measurement results. When detecting calcifications in the tumor anechoic area one obtains stressing of fine calcification echoes, thus increasing the detectability when comparing with the case of healthy breast tissues.

Autorzy przeprowadzili badania wykrywalności zwapienia za pomocą metody ultradźwiękowej cienia i echa przy częstotliwości 5 MHz. Na podstawie rozkładu pola ultradźwiękowego wokół sztywnej kuli wyznaczyli długość cienia, a na tej podstawie warunek wykrywalności dla zwapienia o średnicy $\phi = 3$ mm. W przypadku metody echa, kontynuując poprzednie badania, autorzy ulepszyli technikę pomiarową i rozszerzyli analizę. W celu wyznaczenia tła poziomu zakłóceń tkankowych przeprowadzili pomiary na 82 piersiach zdrowych kobiet przed menopauzą. Granice różnych rodzajów tkanek piersi oraz ich wewnętrzne niejednorodności tworzą zakłócające tło, którego poziom ogranicza wykrywalność zwapienia. Wyniki pomiarów, potwierdzone statystycznie, wykorzystano do wyznaczania wykrywalności w normalnych piersiach (współczynnik tłumienia 1.1 dB/cm MHz). Obliczenia wykazały, że minimalna średnica wykrywalnego metoda echa